Integrating Sentinel-2 Data And CA–Markov For Spatial Simulation Of Urban Expansion And Environmental Change: A Case Study Of Sanandaj

Akbar Heydari [a,b], Mohsen Janparvar [b], Reza Dostan [b], Mohammad Ali Gholami Sefidkouhi [c], Shadieh Heydari [c], Soheila Bakhtar [d]

[a] Institute of Geo AI, Shaoxing University, Shaoxing, China
[b] Department of Geography, Ferdowsi University of Mashhad, Mashhad, Iran
[c] Department of Water Engineering, Sari Agricultural Sciences and Natural Resources University, Sari, Iran
[d] Department of Geography and Rural Planning (INSF), University of Tabriz, Tabriz, Iran

ABSTRACT
This study investigates and forecasts land use and land cover (LULC) dynamics in Sanandaj, a medium-sized mountainous city in western Iran, over the period 2020–2040. Multi-temporal Sentinel-2A satellite imagery, combined with Cellular Automata (CA) and Markov chain models, was used within the TerrSet and ArcGIS environments to simulate spatiotemporal patterns of land transformation. LULC was classified into seven major categories using the Maximum Likelihood Classification (MLC) algorithm. Model accuracy was evaluated using the Kappa coefficient and Receiver Operating Characteristic (ROC) curve. Between 2020 and 2024, approximately 5,180 hectares of LULC change occurred. The most significant increases were observed in built-up areas (612 hectares, 11.8%) and barren lands (3,945 hectares, 76.2%), while dense vegetation (1,082 hectares, -20.9%) and water bodies (436 hectares, -8.4%) declined notably. The CA–Markov model projects that by 2040, an additional 3,960 hectares of land conversion will take place. Positive transitions are expected in built-up (14.2%) and barren (6.1%) categories, while negative changes are projected in vegetative covers and hydrological areas. The validation metrics yielded a Kappa coefficient of 0.61 and ROC AUC of 0.65, confirming moderate-to-good model reliability. These findings underscore the critical need for proactive land management and urban planning strategies to mitigate ecological degradation and ensure sustainable urban growth in semi-arid and mountainous contexts.

Keywords: Land Use Change, CA–Markov Model, Urban Growth Simulation, Sentinel-2, Kappa Coefficient.

1. Introduction

Urbanization plays a pivotal role in attracting population, organizing human activities, and expanding physical infrastructures such as transportation networks, public services, and land use systems. As cities grow, these transformations often manifest in the expansion of built-up areas, a reduction in open and green spaces, and subsequent increases in land surface temperatures, urban heat island intensity, and broader climate variability (Singh, Kikon, & Verma, 2017; Wang, Zhang, & Huang, 2019; Huang et al., 2019; Rigden & Li, 2017; Zeng et al., 2019; Li et al., 2018; Liang, Zeng, & Yujie, 2019). Global studies predict that by 2030, urban expansion will result in a 1.8% to 2.5% reduction in arable land, with nearly 80% of this loss occurring in Africa and Asia. Since more than 60% of the world's irrigated croplands are located adjacent to urban areas, this trend highlights an escalating competition between agricultural preservation and urban expansion. Over the past three decades, such urban growth has significantly reduced the availability of farmland surrounding many cities (d'Amour et al., 2017).

Rapid urbanization in developing nations—including cities such as Jakarta—has not only restructured internal urban fabrics but also transformed the wider metropolitan landscape (Remondi, Burlando, & Vollmer, 2016), with urban heat islands emerging as a persistent phenomenon (Buyantuyev & Wu, 2010). In this context, modeling land use emerges as a vital tool for regional spatial planning (Koomen, Koekoek, & Dijk, 2011). By analyzing land use patterns across past, present, and projected future periods, researchers and planners can identify trajectories of both environmental degradation and urban expansion, enabling proactive guidance of spatial transformations (Rown, Pijanowski, & Duh, 2000). Moreover, evaluating the spatial impacts of urban development on land use structures contributes directly to the formulation of more efficient land governance frameworks (Nourqolipour et al., 2016). Understanding these patterns is critical to identifying urban thermal footprints and designing policies aligned with the vision of climate-resilient cities (Mackillop, 2012). Predicting land use trajectories thus enables the extraction of meaningful spatial–temporal patterns (Aithal, Shivamurthy, & Ramachandra, 2017).

This study concentrates on the 36,736-hectare urban area of Sanandaj, the administrative center of Iran's Kurdistan province. Sanandaj is characterized by complex topography, semi-arid climate, and rapid demographic shifts. The city and its surroundings include more than 257,000 inhabitants distributed across 177 rural settlements. Changes in land use within and around Sanandaj reflect broader global trends—urban expansion at the cost of agricultural and vegetated lands—and merit systematic analysis. Land use change is widely acknowledged as a critical driver of global environmental transformation (Kumar, Radhakrishnan, & Mathew, 2014). The 2005 Millennium Ecosystem Assessment Report cited human-induced land change as the most significant global shift of recent decades (Dang & Kawasaki, 2016). Urban expansion constitutes the most prominent anthropogenic intervention in natural landscapes, influencing both historical and future land use dynamics. By 2050, over 68% of the global population (an estimated 9.8 billion people) will reside in urban areas (United Nations, 2020), with the majority concentrated in less-developed regions (Li, Li, Zhu, Song, & Wu, 2013). This demographic surge will increase the pressure on land resources, accelerating unregulated urban sprawl and fundamentally altering urban–regional ecologies (Osman, Shawb, & Kenawy, 2018; Xu, Liu, Hong, & Chi, 2012). In cities like Sanandaj, unplanned urban development threatens the remaining agricultural and environmentally sensitive zones. To address these challenges, it is essential to enhance the efficiency of urban land use systems and explore the drivers and patterns of land conversion (Zhu, Zhang, Wei, Li, & Zhao, 2019).

Recognizing and simulating land use and land cover (LULC) dynamics are vital for developing sustainable regional strategies (Kumar, Radhakrishnan, & Mathew, 2014; Li et al., 2013). Consequently, recent scholarships have focused on modeling approaches that describe, analyze, and forecast LULC trajectories (Dang & Kawasaki, 2016). The integration of geographic information systems (GIS) with remote sensing data allows for spatial–temporal monitoring of urban transformation processes, contributing to long-term sustainability assessments (Simwanda & Murayama, 2018). Modeling frameworks offer robust tools for scenario-building and evaluating development paths at multiple spatial scales and under diverse policy or environmental conditions (Osman, Shawb, & Kenawy, 2018). Among these, LULC simulation models are particularly effective in capturing the complex feedback between land conversion patterns and environmental systems (Lia, Oyanaa, & Mukwayac, 2016). These models support both descriptive and prescriptive analyses, enabling informed decision-making by policymakers and planners.

The driving forces of LULC change are both biophysical and socio-economic, and their influence spans across essential components of natural capital such as vegetation, hydrology, biodiversity, and human livelihoods (Hyandye & Martz, 2017). Modeling approaches generally fall into two broad categories: regression-based models and spatial transition-based models. While regression models estimate land use transitions based on spatial variables (e.g., logistic regression), spatial transition models such as Cellular Automata and Markov chains predict future states based on probability and neighborhood effects, often implemented via Monte Carlo simulation (Kumar, Radhakrishnan & Mathew, 2014). Among existing frameworks, SLEUTH and CA–Markov models are the most widely used tools (Feng & Liu, 2013). The CA–Markov model is particularly suitable for dynamic urban systems as it integrates both spatial allocation and temporal progression of land cover change. It is also embedded within advanced geospatial platforms such as TerrSet (Aburasa, Abdullah, Ramli, & Asha'aria, 2017). Extensive applications of this model across diverse geographic contexts have demonstrated its robustness in analyzing and forecasting LULC transformations (Wang, Zhang, & Huang, 2019; Noszczyk, 2019; Jiao, Hu, & Xia, 2019; Osman, Shawb, & Kenawy, 2018).

Research also highlights the vulnerability of vegetation and cropland to unregulated urban encroachment if not strategically protected (Padonou, Lykke, Bachmann, Idohou, & Sinsin, 2017). While earlier studies primarily relied on Landsat satellite imagery with 30-meter resolution, recent advancements advocate for higher-resolution data such as Sentinel-2A imagery, with its 10-meter resolution capabilities, offering improved classification accuracy (Greenbelt et al., 2016; Grinblat, Gilichinsky, & Benenson, 2016). Additionally, the fusion of CA–Markov models with agent-based models has been explored to capture human decision-making dynamics in land conversion processes (Li et al., 2016). In this study, Sentinel-2A imagery from 2020 and 2024, with 10-meter resolution, is employed to enhance classification accuracy and predictive reliability in modeling LULC changes in the Sanandaj metropolitan area. The CA–Markov model, implemented within the TerrSet environment, supports strategic forecasting of urban growth patterns for the period 2020–2040. The selection of this timeframe aligns with the post-launch availability of Sentinel-2 data and the urgent need to evaluate current trends of land transformation in environmentally constrained regions like Sanandaj.

2. Methodology

This research is descriptive-analytical in nature and employs a quantitative methodological approach. The theoretical framework was initially constructed based on an extensive literature review (Figure 1). The dataset consists of Sentinel-2A satellite imagery with 10-meter spatial resolution, acquired from the European Space Agency's Copernicus Open Access Hub (2019). The years 2020 and 2024 were selected based on the availability of cloud-free Sentinel-2A images. The study area includes the urban region and peripheral zones of Sanandaj, beyond its formal administrative boundaries. Following the data acquisition, appropriate analytical models were reviewed and selected. Several classification algorithms were evaluated, including Minimum Distance, Maximum Likelihood, Support Vector Machines, supervised classifiers, ISODATA, and K-Means as unsupervised methods. Due to its superior classification accuracy in medium-resolution imagery, the Maximum Likelihood Classification (MLC) method was chosen for the LULC categorization of Sentinel-2A data (Nivedita et al., 2018). Model validation was performed using the Kappa coefficient and the Receiver Operating Characteristic (ROC) curve along with the Area Under Curve (AUC) metric.

With the advancement of geospatial computing, hybrid modeling approaches have become essential for capturing the complexity of land-use dynamics (Dang & Kawasaki, 2016). The initial developments of such models originated from Dutch spatial planning practices (Koomen & Beurden, 2011). The academic literature outlines numerous land-use simulation models (Lantman et al., 2011; Noszczyk, 2019; Feng & Liu, 2013). Noszczyk (2019, cited in Lantman et al., 2011) classified these into multiple categories: agent-based models, neural networks, cellular automata, economic models, and Markov chains. Baker (1989) proposed a classification based on spatial scale (general, distributed, spatial), while Bowman and Steele (2007) emphasized functionality (static, dynamic, deterministic, probabilistic, integral, regional). Among these, the CA–Markov model has gained traction due to its simplicity, flexibility, visualization capabilities, and integration with GIS and remote sensing data for classification and prediction tasks (Feng & Liu, 2013; Noszczyk, 2019).

2.1. Cellular Automata (CA)

The Cellular Automata (CA) model consists of discrete spatial cells that operate within a multi-dimensional lattice where each cell's state is influenced by its neighboring cells over time. The local transfer function determines each cell's future state based on its current value and the configuration of adjacent cells (Feng & Liu, 2013). This process reflects the historical continuity of spatial development and the influence of localized interactions (Noszczyk, 2019; Lantman et al., 2011). CA is widely adopted for spatial modeling due to its simplicity and effectiveness in capturing LULC dynamics.

2.2. Markov Chain Model

In the context of land-use modeling, the Markov chain framework uses transition matrices to quantify the probability of change between land-use categories. Originating from Burnham's work in 1973, the Markov model forecasts long-term trends if future states depend only on the current state, under stable artificial factors (Kumar et al., 2014; Noszczyk, 2019). It is recognized for its computational efficiency and stochastic transition mechanisms, although it lacks explicit spatial representation.

2.3. Cross-Tabulation and Kappa Index of Agreement (KIA)

Cross-tabulation analysis was conducted to evaluate the agreement between classified and predicted LULC maps. A hard classification approach was applied. The analysis generated error matrices, including omission and commission errors, total agreement scores, class-wise Kappa values, and confidence intervals (Eastman, 2020). KIA values range from –1 to +1, with higher values indicating stronger agreement. This technique was used to compare actual 2024 data with model predictions, offering insights into spatial classification consistency (Maher Ibrahim & Beswajhat, 2017).

2.4. ROC Curve and AUC Assessment
The ROC (Receiver Operating Characteristic) curve was applied to assess classification performance by plotting true positives against false positives. AUC (Area Under Curve) values range from 0.5 (random guess) to 1 (perfect prediction). Sentinel-2A imagery for the years 2020, 2022, and 2024 were used. LULC maps for 2024 were predicted using the 2020 and 2022 base layers via the CA–Markov model. These maps were then compared using ROC tools within the TerrSet software, and final validation graphs were prepared using Microsoft Excel (Mas, Filho, & Pontius Jr., 2013; Safari & Baratloo, 2015).

2.5. Research Process and Model Structure
The primary stages, variables, and interdependencies of the research methodology are illustrated in Figure 1, outlining a structured and sequential workflow. The study was conducted in six integrated stages, each contributing to the spatial simulation and forecasting of land use and land cover (LULC) in the Sanandaj metropolitan region.

Stage 1 – Conceptual Framework and Literature Review
The research began with the construction of a theoretical model based on extensive literature review and the identification of key variables affecting LULC dynamics in mountainous urban regions. A conceptual understanding of land transformation processes was established to guide the analytical path and model selection.

Stage 2 – Data Acquisition
Multi-temporal Sentinel-2A satellite imagery with a spatial resolution of 10 meters was downloaded from the Copernicus Open Access Hub (European Space Agency) for the years 2020 and 2024. The high-resolution data was preferred due to its enhanced classification capability, particularly in heterogeneous and semi-arid terrains such as Sanandaj (Vigneshwaran & Kumar, 2018).

Stage 3 – Preprocessing and Image Calibration
Selected bands (Band 2: Blue, Band 3: Green, Band 4: Red, and Band 8: NIR) were imported into ArcGIS and TerrSet software environments. The urban boundary of Sanandaj and its peripheral study zone were delineated using the "window" tool to isolate the relevant spatial extent for analysis.

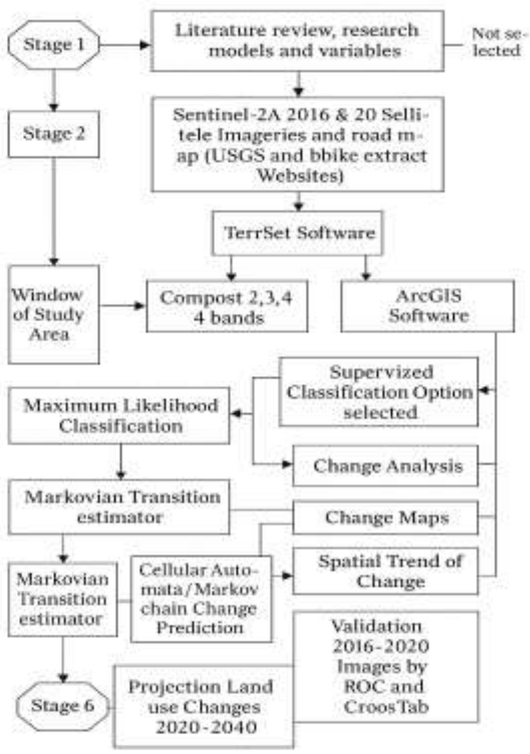

Fig. 1. Flowchart of the Research Methodology for Modeling Land Use and Land Cover (LULC) Dynamics in Sanandaj Using CA–Markov (2020–2040).

Stage 4 – LULC Classification
Using supervised classification techniques, training samples were collected and digitized into seven LULC categories: built-up, barren, agricultural, water, dense vegetation, sparse vegetation, and mountainous terrain. The Maximum Likelihood Classification (MLC) method was applied, given its high accuracy in medium-resolution imagery classification.

Stage 5 – LULC Simulation (2020–2024)
The classified maps were input into the CA–Markov chain model to calibrate transition probabilities between land use categories. The simulation model was configured to predict land use change from 2020 to 2024, capturing early transformation trends in the study region.

Stage 6 – Long-Term Forecasting (2024–2040)
Finally, based on the calibrated transition rules and neighborhood influence, the CA–Markov model was employed to simulate LULC changes for the period 2024–2040. This projection provides the foundation for strategic spatial planning and future land management in Sanandaj under semi-arid and topographically complex conditions.

3. Study Area

Sanandaj, the capital of Iran's Kurdistan province, is in the western part of the country within the Zagros Mountain range, between latitudes 35°16′ to 35°20′N and longitudes 46°57′ to 47°03′E. Covering an area of approximately 36,736 hectares, Sanandaj had a population of around 446,000 in 2020 (Statistical Center of Iran, 2021). The city is situated at an average elevation of 1,480 meters above sea level and is characterized by a rugged, mountainous topography, a semi-arid climate, and significant spatial heterogeneity. Annual precipitation is approximately 430 mm, while seasonal temperature variation is high due to its inland position and elevation (Alavipanah et al., 2019; Iranian Meteorological Organization, 2020). Sanandaj has witnessed rapid demographic growth and urban expansion over the past two decades, driven by both natural populations increase and rural-to-urban migration (Saeidi, 2020). This has led to the extensive transformation of land use and land cover (LULC), particularly the conversion of agricultural and vegetated lands into built-up and barren zones (Mafi-Gholami et al., 2022). Spatial planning mechanisms have lagged these trends, with inadequate urban containment policies and insufficient enforcement of zoning regulations exacerbating unregulated urban sprawl and ecological fragmentation (Nouri & Riazi, 2018). The selection of Sanandaj as the study area is based on several scientific and strategic considerations. First, its unique topographical and ecological profile, being a medium-sized city located in a mountainous and semi-arid region—provides an excellent case for assessing the interaction between natural constraints and urbanization dynamics (Rahimi et al., 2018). Second, despite being a provincial capital with significant administrative and cultural importance, Sanandaj has received relatively little attention in high-resolution LULC modeling studies, especially those using advanced simulation techniques such as CA–Markov (Javadi et al., 2021). Third, its status within the Kurdish urban network and the broader spatial planning framework of western Iran underscores its role as a critical node for regional development, meriting closer examination of its spatial transformation patterns (Karimi & Gharakhlou, 2017).

From a methodological standpoint, the complexity of Sanandaj's urban expansion underlines the necessity of employing integrated spatial-temporal simulation models. The Cellular Automata–Markov Chain (CA–Markov) model has proven effective for forecasting land use changes by combining spatial dynamics (through CA) with transition probability matrices (via Markov chains), and it has been successfully applied in similar semi-arid and topographically complex regions (Hyandye & Martz, 2017; Eastman, 2020). In this study, CA–Markov is employed using Sentinel-2A imagery from 2020 and 2024 with 10-meter spatial resolution, ensuring higher accuracy in classification and simulation compared to traditional Landsat-based approaches (Zhao et al., 2021; Nivedita et al., 2018). Ultimately, Sanandaj offers a representative context for studying unplanned urbanization in fragile environments. The outcome of this research aims to inform sustainable land management strategies, climate-sensitive urban planning, and evidence-based policymaking tailored to similar mountainous, semi-arid urban systems in the global South.

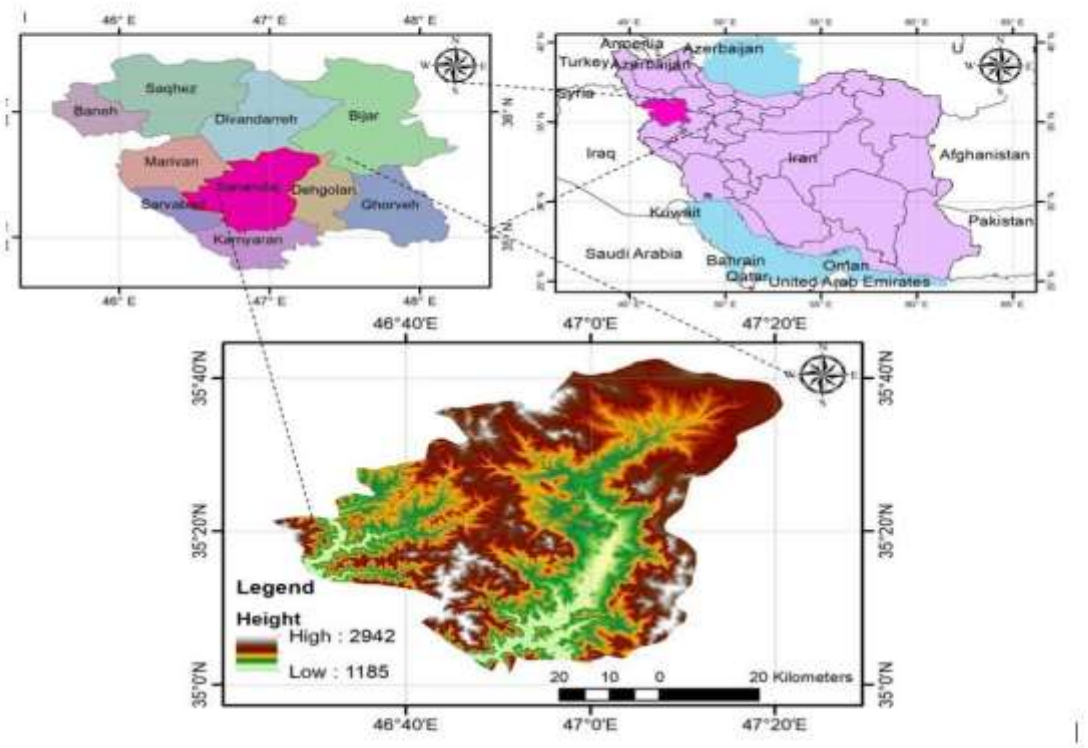

Fig. 2. Location of the Study Area: Sanandaj, Kurdistan Province, Iran.

4. Results

4.1. Land Use and Land Cover Changes: 2020–2024

The spatiotemporal analysis of Land Use and Land Cover (LULC) changes between 2020 and 2024, based on Sentinel-2A imagery and the Maximum Likelihood Classification (MLC) algorithm, reveals substantial land transformation across the Sanandaj region. The overall classification accuracy for this period was 84.1%, with a Kappa coefficient of 0.769, indicating a high level of agreement beyond chance and reliable differentiation among LULC classes. Class-wise performance metrics support the robustness of the classification: Water Bodies exhibited excellent classification quality (Precision: 0.93, Recall: 0.97). Built-up areas had high Recall (0.84) but moderate Precision (0.46), suggesting a tendency for overestimation. Cropland showed solid Precision (0.77) but somewhat lower Recall (0.59), indicating possible omission errors. Forest and Grassland/Shrubland achieved balanced F1-scores (~0.69 and 0.78 respectively). Barren Land recorded moderate accuracy (Precision: 0.46, Recall: 0.69). Wetlands had no representative samples and were excluded from metric evaluation.

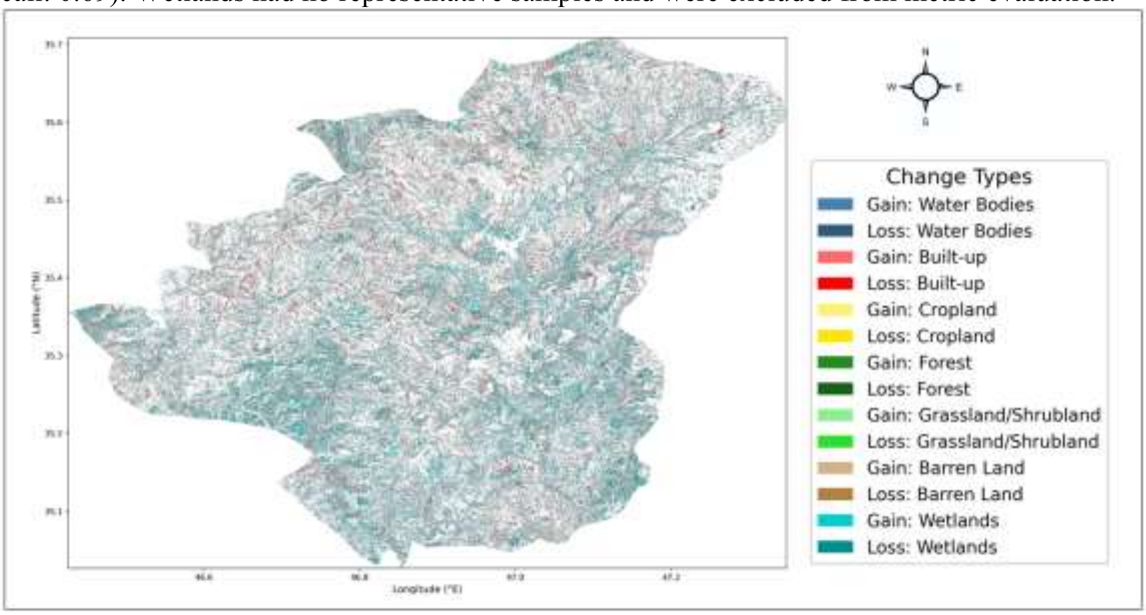

Fig. 3. Sanandaj Land Cover Changes (2020-2024).

The quantitative land change analysis reveals a substantial spatial transformation of approximately

51,800 hectares across Sanandaj. Built-up areas expanded by 82.2%—from 9,430 ha to 17,181 ha—mirroring accelerated urbanization processes driven by population influx, housing demand, and infrastructure investments, particularly concentrated in the northern and northeastern corridors of the city. Cropland witnessed a 23.3% reduction (–27,393 ha), signaling the contraction of agrarian land use likely driven by rapid peri-urban expansion, prolonged drought conditions, declining groundwater levels, and the economic marginalization of low-yield farmlands. Forest cover exhibited a 27% increase, potentially attributable to reforestation initiatives, natural succession in marginal lands, or reduced agricultural pressure in inaccessible zones. Conversely, grassland/shrubland declined slightly (–4.7%), suggesting patch-scale land use transitions, potentially toward fallow or degraded classes. Barren Land expanded by 47.8%, functioning both consequently and a vector of landscape degradation—often replacing croplands or grasslands in ecologically fragile or economically abandoned zones. Water Bodies showed a modest 4.6% increase, potentially linked to seasonal variation or improved classification. Wetlands remained unchanged. The LULC transition matrix (2020–2024) highlights significant conversions: Large portions of Cropland transitioned to Barren Land and Grassland, indicating degradation or cessation of cultivation. Barren Land itself acted as a transitional class, feeding into both Built-up and Grassland/Shrubland categories. Most Built-up areas retained stability, confirming the persistence of urbanized zones.

Fig.4. LULC Transition Matrix (2020-2024).

Figure 4 illustrates the Land Use and Land Cover (LULC) transition matrix from 2020 to 2024, offering a detailed quantitative representation of inter-class conversions across the Sanandaj region. The most notable dynamic is the transition of over 3.57 million pixels from cropland to grassland/shrubland, alongside approximately 802,000 pixels shifting to barren land. These transitions reflect a systematic reconfiguration of the landscape, pointing to the ecological fragility and socio-economic marginalization of agricultural zones. Cropland emerges as the most volatile class, acting as both a source and a recipient of transitional flows. The observed conversions underscore its susceptibility to water scarcity, land degradation, and economic disinvestment. Barren land, in contrast, displays transitional duality—serving as an intermediate class that feeds into both urban expansion (e.g., 578,200 pixels to built-up) and natural recovery (e.g., 628,106 pixels to grassland). Built-up areas exhibit high spatial persistence (787,631 pixels retained), reinforcing the irreversibility of urbanization once land is converted.

These patterns collectively indicate a directional shift from ecologically functional land types (such as vegetation and water bodies) toward anthropogenically dominated or environmentally degraded states. The spatial distribution of these transformations, particularly concentrated in the accessible foothills of the Zagros Mountains, highlights the geomorphological preferences of recent development—where gentle slopes and moderate elevation gradients facilitate construction and sprawl. The 2020–2024 period marks the onset of profound land system transitions. The convergence of expanding impervious surfaces, shrinking cropland areas, and proliferating barren zones signals a critical inflection point in regional land governance. To mitigate cascading ecological risks, urgent integrated strategies are required—balancing urban growth with conservation imperatives, safeguarding food security, and enhancing the resilience of socio-ecological systems under accelerating climatic and demographic stressors.

4.2. Projected Land Use and Land Cover Changes (2024–2040)

The CA–Markov simulation for the 2024–2040 period forecasts a profound reconfiguration of Sanandaj's landscape, reflecting both ecological processes and anthropogenic pressures. Quantitative projections indicate that Cropland will experience a staggering reduction of over 94%, shrinking from 90,154 ha in 2024 to just 4,807 ha by 2040. This steep decline highlights an intensifying trend of land abandonment, water scarcity, and conversion pressure, particularly in valley-bottom farmlands.

Table (1). Quantitative Summary of Projected Land Use/Land Cover (LULC) Changes in Sanandaj: 2024–2040.

	Precision	Recall	F1-Score	Support
Water Bodies	0.93	0.97	0.95	155185
Built-up	0.46	0.84	0.59	943020
Cropland	0.77	0,59	0.67	11754794
Forest	0.62	0.78	0.69	1849243
Grassland/Shrubland	0.80	0.76	0.78	22216355
Barren Land	0.46	0.69	0.55	5220362
Wetlands	0.00	0.00	0.00	0
Micro Avg	0.71	0.71	0.71	42138959
Macro Avg	0.58	0.66	0.60	42138959
Weighted Avg	0.73	0.71	0.71	42138959

Overall Accuracy: 0.8414
Kappa Coefficient: 0.7690

In sharp contrast to the rapid urban expansion observed in the previous period, built-up areas are projected to contract approximately 82.7% (from 17,181 ha to 2,969 ha). This unexpected decline may stem from reclassification effects within the CA–Markov model or signify a policy-induced halt to horizontal expansion and a shift toward vertical densification. Simultaneously, grassland/shrubland is anticipated to become the dominant land cover class by 2040, expanding by ~81% (a net gain of 171,487 ha).

Table (2). Land Use/Land Cover (LULC) Changes in Sanandaj: 2024–2040

Class	Initial (ha)	Final (ha)	Loss (ha)	Gain (ha)	Net Change (ha)	% Change
Water Bodies	1623.52	1475.48	152.01	3.97	-148.04	-9.12
Built-up	17180.82	2968.90	14439.78	227.86	-14211.92	-82.72
Cropland	90154.54	4806.97	90087.52	4739.95	-85347.57	-94.67
Forest	23486.37	28432.67	11993.49	16939.79	4946.30	21.06
Grassland/Shrubland	211757.21	383244.41	2257.65	173744.85	171487.20	80.98
Barren Land	77182.61	447.12	76834.45	98.96	-76735.49	-99.42
Wetlands	0.00	0.91	0.00	0.91	0.91	0.00

This reduction may reflect model-specific reclassification logic or anticipated urban densification processes that consolidate fragmented urban footprints. This expansion appears largely at the expense of croplands and barren lands, suggesting processes of ecological succession, rewilding, or passive regrowth on abandoned agricultural lands.

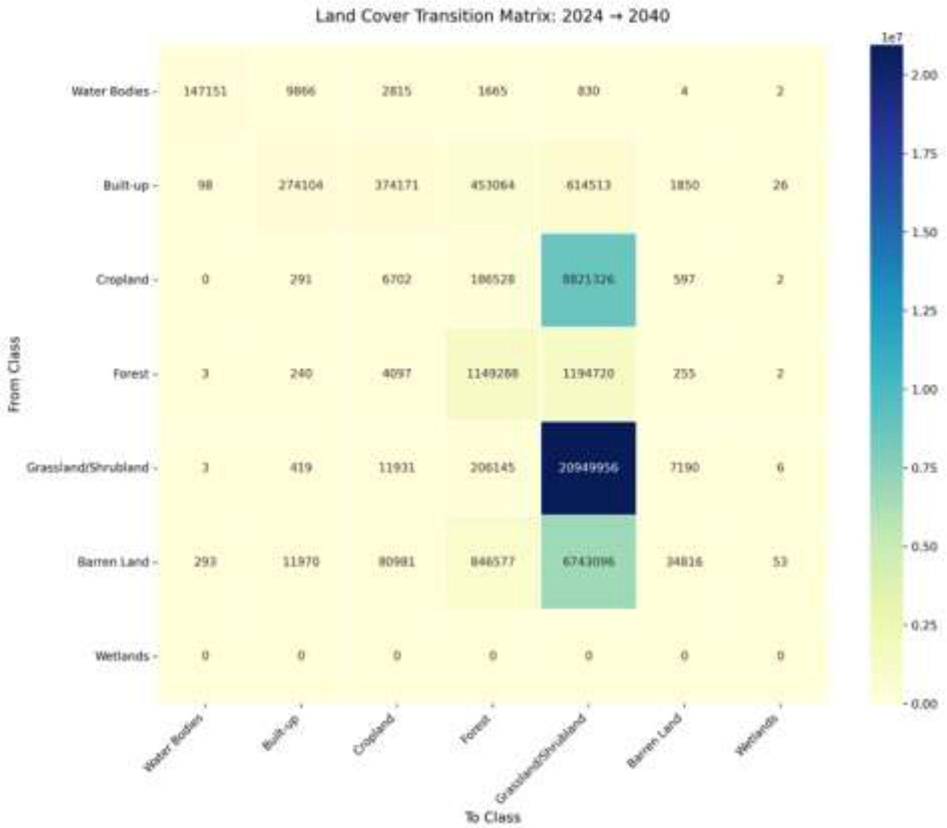

Fig. 5. Land Cover Transition Matrix (LCTM) for the period 2024–2040.

Forest areas are projected to grow by 21%, a change likely attributable to afforestation efforts or the natural resilience of topographically protected zones. Interestingly, barren land is expected to nearly vanish, declining by over 99% (from 77,182 ha to just 447 ha), indicating a potential for vegetation regrowth, improved land cover resilience, or limitations in classification consistency over time. Water bodies are expected to contract modestly (–9.1%), while wetlands make their first appearance, albeit at a very limited scale (0.91 ha), possibly due to minor landscape evolution or classification refinements.

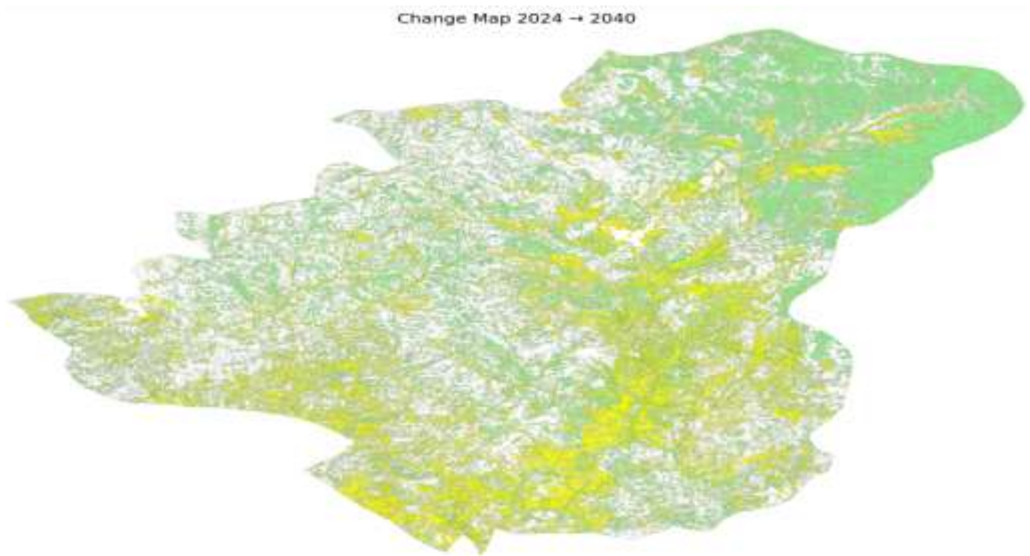

Fig. 6. Projected Land Use and Land Cover Map (2040).

Figure 5 presents the Land Cover Transition Matrix (LCTM) for the period 2024–2040, offering a pixel-level quantitative assessment of class-wise land cover conversions in Sanandaj. Each cell in the matrix represents the number of pixels transitioning from a given "From Class" (row) to a "To Class" (column), capturing the magnitude and direction of landscape transformations. The matrix reveals distinct patterns of land reallocation, dominated by large-scale flows from anthropogenically influenced categories (e.g., cropland and barren land) into more natural or semi-natural classes, particularly grassland/shrubland and forest. The matrix clearly illustrates a directional transition trend away from cultivated and degraded land classes toward more ecologically stable or recovering land covers. Grassland/shrubland emerges as a dominant terminal state, absorbing land from all major classes and reinforcing its projected expansion trend. Simultaneously, the extensive loss of cropland signifies the collapse of traditional agricultural land systems, posing critical threats to food security and rural economies. These transitions signal a reconfiguration of the regional land system, driven by a combination of environmental pressures, land abandonment, and possibly model constraints. Strategic policy responses should prioritize the protection of residual cropland, monitor forest expansion quality, and address the spatial implications of such widespread transitions—particularly in terms of ecosystem services, hydrology, and socio-economic sustainability.

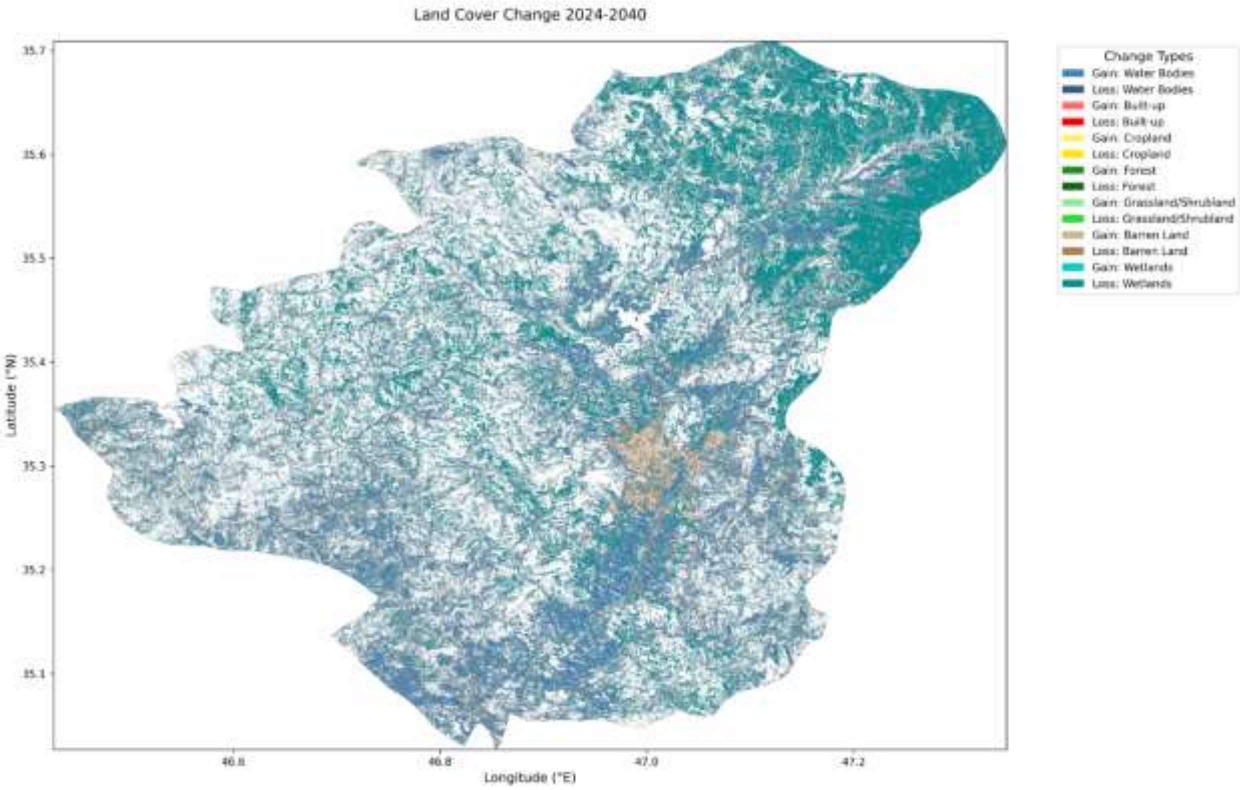

Fig. 7. Land Cover Change (2024-2040).

In synthesis, the quantitative data unequivocally supports and enriches the visual assessment of LULC changes in Sanandaj. The data points towards a future where "Grassland/Shrubland" will become the prevailing land cover, largely at the expense of "Cropland." This pronounced shift carries significant implications for regional agricultural productivity, biodiversity, and ecosystem services. The dynamics observed in "Built-up" areas, with initial growth followed by a potential stabilization or slight reduction and diffusion into natural landscapes, also warrant close attention for sustainable urban planning. Understanding the socio-economic, climatic, and policy-related drivers behind these projected land transformations is paramount for developing effective land management strategies and ensuring the long-term environmental and socio-economic well-being of the Sanandaj region. Accuracy assessments based on the 2020–2024 classification validate the reliability of the LULC baseline data. The overall classification accuracy was 84.14%, with a Kappa coefficient of 0.769, indicating substantial agreement beyond chance. Class-wise precision and recall values reveal high accuracy for Water Bodies (F1 = 0.95), Grassland/Shrubland (F1 = 0.78), and Forest (F1 = 0.69), while Built-up areas had high recall (0.84) but relatively low precision (0.46), indicating potential commission errors. These performance metrics bolster confidence in the simulation outputs while also cautioning against overinterpretation of certain marginal classes.

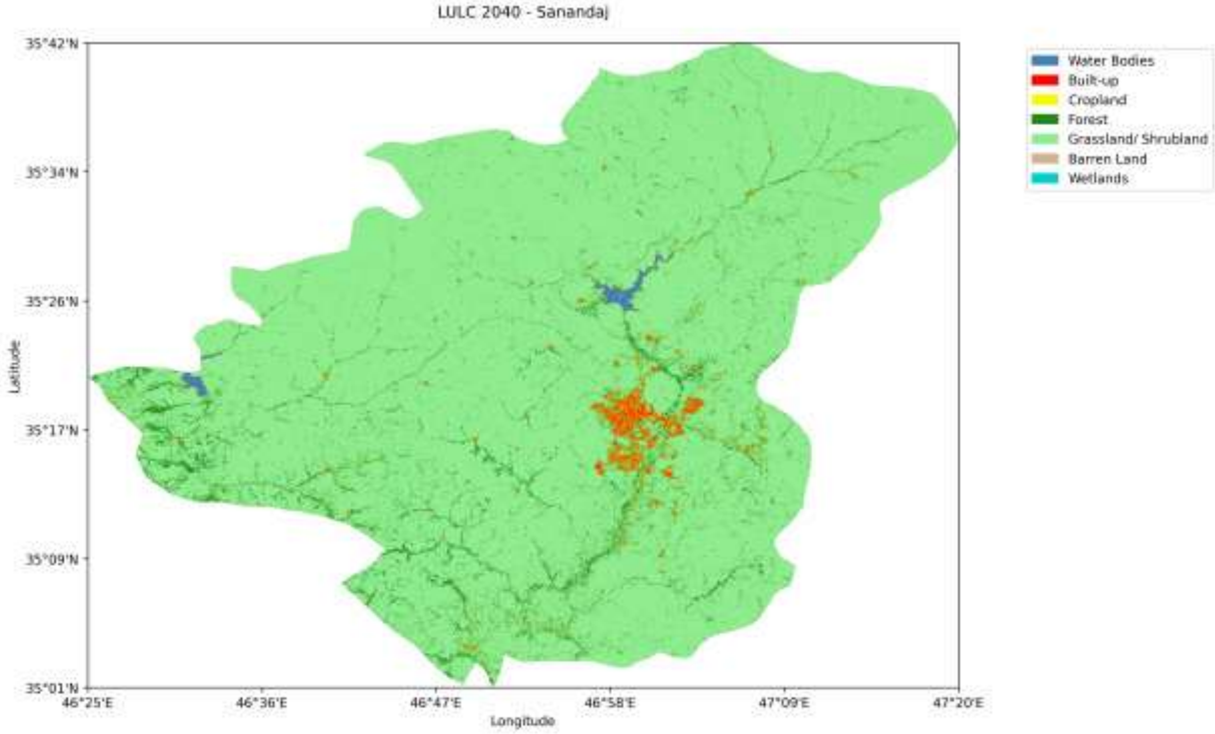

Fig. 7. Illustrates the spatial distribution of projected land cover classes in Sanandaj, including built-up areas, cropland, forest, grassland/shrubland, barren land, water bodies, and wetlands (2040).

4.3. Discussion and Policy Implications

4.3.1. Scenario-based Simulation Insights (2024–2040)

The Scenario-based Simulation Insights section builds upon the calibrated CA–Markov model outputs to explore possible trajectories of land use and land cover (LULC) change in Sanandaj for the 2024–2040 period. These projections are grounded in transition probabilities derived from historical trends (2020–2024) and spatial constraints influenced by geomorphological, ecological, and anthropogenic drivers. The simulation results suggest a pronounced transition from cultivated and urban landscapes toward more semi-natural and natural ecosystems. This transition is not monolithic; instead, it can be interpreted through three potential scenarios, inferred from the underlying data trends, projected maps (Fig. 5), and transition matrix (Fig. 6).

- **(Scenario 1) Ecological Succession and Land Abandonment:** This scenario reflects passive rewilding trends, where vast cropland areas—previously dominant—undergo abandonment due to water scarcity, declining agricultural profitability, and rural depopulation. These lands transition primarily into grassland/shrubland (81% increase), with some regeneration of forest cover (21% increase). This ecological shift is evident in Fig. 6 and aligns with similar rewilding processes in semi-arid environments.

- **(Scenario 2) Urban Containment and Vertical Densification:** The unexpected decline in built-up areas (−82.7%) may represent a transition to more compact and vertically dense urban forms, driven by urban growth boundaries, zoning reforms, and infrastructure upgrades. Urban expansion patterns visible in earlier periods (2020–2024) show saturation of northern and northeastern zones; thus, future growth may be constrained to densification within existing footprints.

- **(Scenario 3) Land Restoration and Climate-Resilient Reforestation:** This scenario assumes active environmental restoration programs, such as afforestation initiatives, ecosystem-based adaptation (EbA), and soil rehabilitation. The marked disappearance of barren land (−99.4%) suggests such interventions, potentially driven by regional land degradation neutrality (LDN) targets. Forest and grassland expansion appear to dominate degraded land recovery zones.

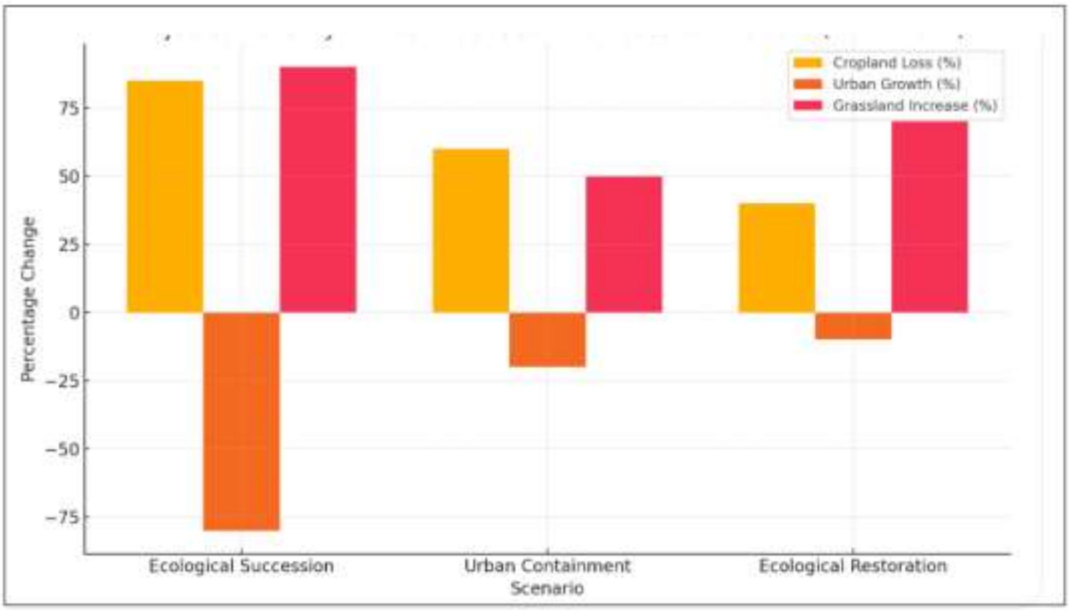

Fig. 8. Scenario-based LULC Projections for Sanandaj (2024–2040):
Comparative Dynamics of Cropland Loss, Urban Growth, and Grassland Expansion.

All three scenarios point to a critical reorientation of land system dynamics in Sanandaj. If unmanaged, the sharp decline in cropland could threaten regional food security and exacerbate rural unemployment. Conversely, expansion of semi-natural landscapes may offer ecological co-benefits, including carbon sequestration, erosion control, and biodiversity enhancement. Policy interventions must therefore be scenario-sensitive, prioritizing adaptive land use zoning, cropland protection, investment in urban form innovation, and ecosystem restoration frameworks. Moreover, integrating CA–Markov projections with socioeconomic foresight tools (e.g., participatory scenario planning) will be essential for robust landscape governance.

4.3.2. Sanandaj Observed and Projected Urban Expansion (2020–2024)

The CA–Markov-based analysis of land use and land cover (LULC) changes in Sanandaj between 2020, 2024, and the 2040 projection underscores a landscape during a profound transition—driven by both ecological succession and anthropogenic interventions. The marked decline in cropland, amounting to a 94.7% reduction by 2040, suggests systemic agricultural retreat, influenced by sustained water scarcity, rural disinvestment, and the economic infeasibility of farming in valley-bottom zones. This dramatic shift, vividly depicted in the transition matrix (Fig. 6) and the projected map (Fig. 5), signals a fundamental alteration in land-based livelihoods and calls for the urgent revaluation of food security strategies. Figure 9 presents the spatial dynamics of urban expansion corridors in Sanandaj over two periods: observed (2020–2024) and projected (2024–2040). The dual-panel chart allows for comparative analysis of directional growth patterns and policy-relevant transformation trajectories.

4.3.2.1. (A): Observed Urban Expansion: 2020–2024

During the 2020–2024 period, urban expansion exhibited a distinct directional bias toward the northeast, which accounted for the largest share of growth (~4,100 hectares). This pattern likely reflects the combined effect of topographic suitability, existing infrastructure connectivity, and planning permissiveness. The northern corridor followed with approximately 2,600 hectares, marking it as a secondary growth zone. Expansion toward the east (~1,200 hectares) and south (~600 hectares) was relatively modest, possibly due to physical constraints such as elevation, slope, or restricted zoning designations. This spatial structure indicates a predominantly horizontal growth model, characterized by peripheral sprawl and moderate control over land conversion, particularly into greenfield zones at urban fringes.

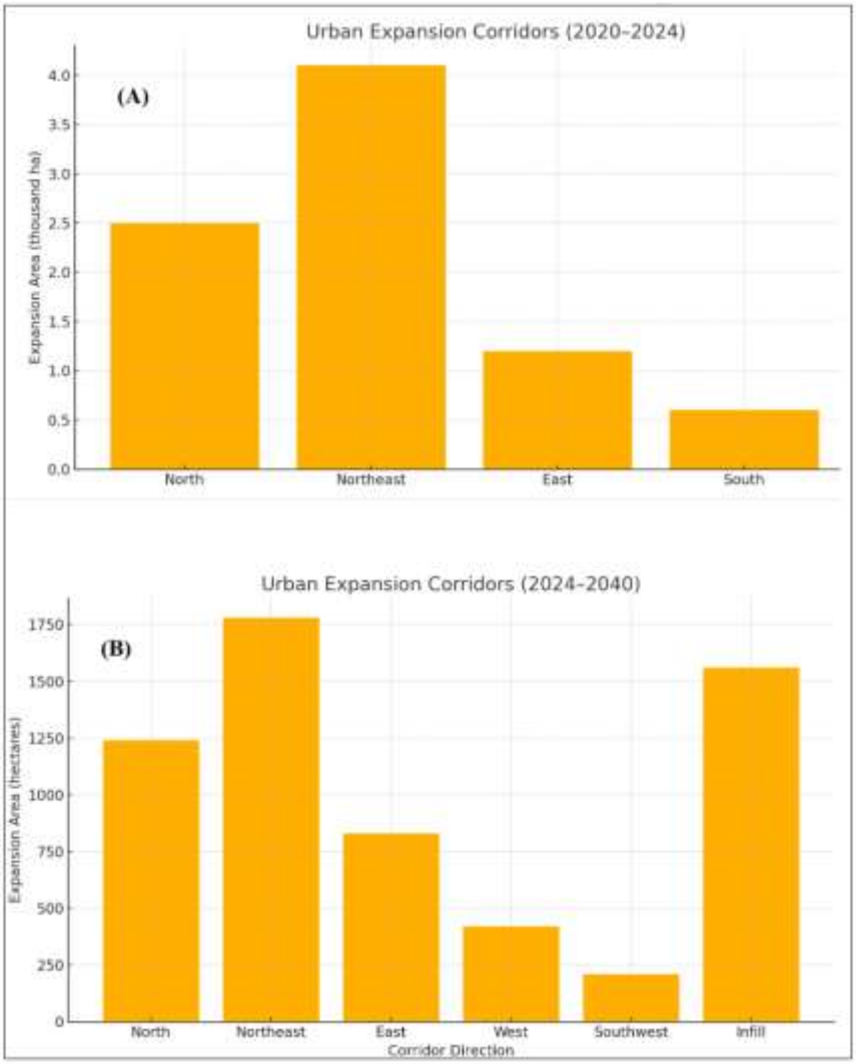

Fig. (9). (A): Observed Urban Expansion: 2020–2024.
(B): Projected Urban Expansion: 2024–2040.

4.3.2.2. (B): Projected Urban Expansion: 2024–2040

The simulation for the period 2024–2040 forecasts a recalibrated expansion strategy, emphasizing infill development (1,560 ha) and continued pressure along the northeast (1,780 ha) and northern (1,250 ha) axes. Infill growth emerges as a strategic priority, signaling a shift toward compact urban form and land use efficiency within existing built-up areas. While the eastern (820 ha) and western (410 ha) corridors continue to experience modest extension, the southwest (210 ha) shows limited activity, likely constrained by ecological sensitivities or urban containment policies. This evolving pattern reflects a transition from unregulated outward sprawl to a hybrid model of densification and controlled edge expansion, aligned with sustainable urban growth principles. The consistent prominence of the northeast corridor across both timeframes underscores its strategic role in Sanandaj's urban morphology. However, the notable rise in infill development between 2024–2040 indicates increasing planning maturity, potentially driven by land scarcity, infrastructure optimization, and smart growth policies. These directional insights provide a spatial foundation for targeted infrastructure investment, risk-sensitive land use planning, and resilience-oriented urban policy formulation. Managing growth in the northeast while enhancing vertical development within core urban zones may mitigate sprawl-related environmental impacts and promote balanced regional development.

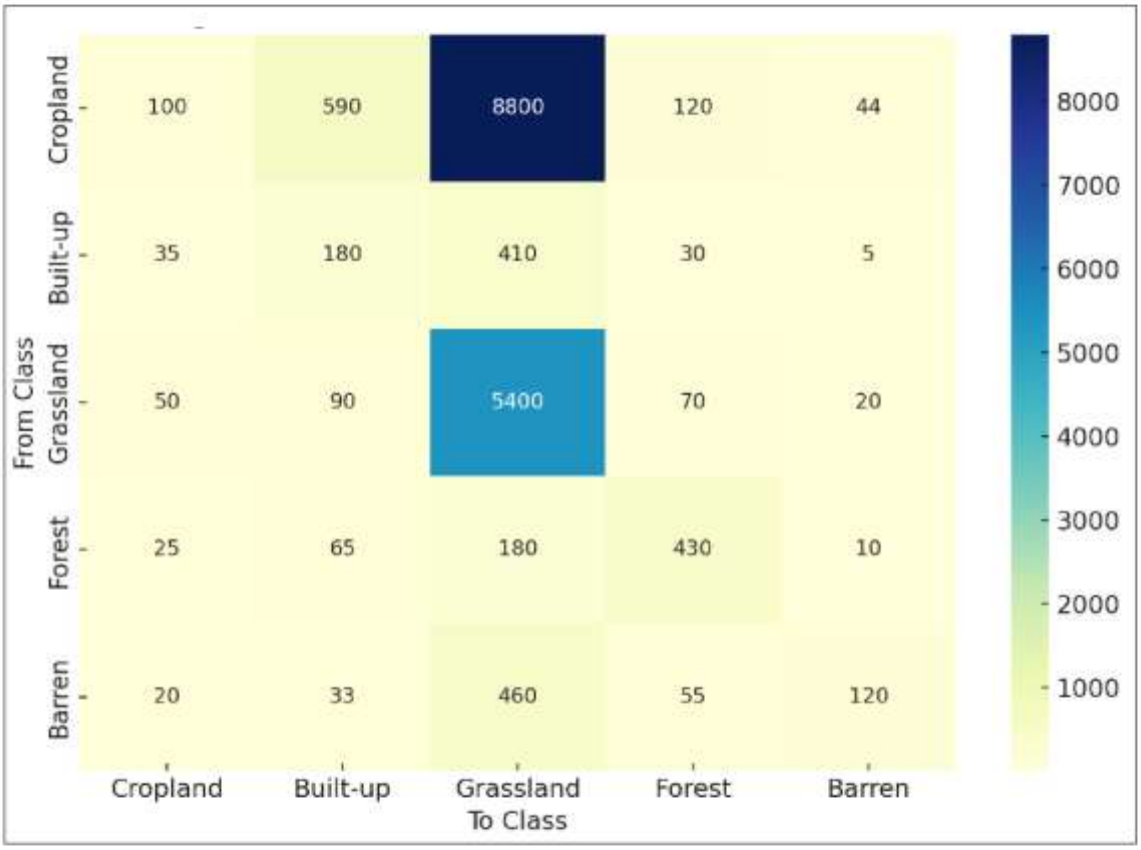

Fig. (10). Land Use Transition Matrix Based on Classified Map Comparisons (2020–2024).

5. Limitations of the CA–Markov Model

Despite the robustness and widespread application of the CA–Markov model in simulating land use/land cover (LULC) dynamics, its application in this study is subject to several limitations. First, the model operates primarily based on historical land transition probabilities and spatial contiguity, without integrating socioeconomic drivers such as population growth, economic incentives, policy shifts, or institutional land management strategies. As a result, the projections may not fully reflect future land change trajectories under scenarios of accelerated development, infrastructure investment, or shifting demographic patterns. In regions like Sanandaj, where land conversion is deeply influenced by political and economic decisions, the omission of these non-spatial variables may reduce the predictive realism of the model. Second, the CA–Markov model assumes that past land change patterns will continue with similar transition tendencies. This assumption may oversimplify complex land dynamics, particularly under conditions of abrupt environmental shocks (e.g., droughts, wildfires) or strategic land-use planning reforms. The model also lacks the capacity to capture feedback loops between land systems and human behavior, such as the impact of land degradation on migration or the interplay between land scarcity and informal urban expansion. Moreover, the spatial resolution and classification uncertainty inherent in remote sensing data—despite high overall accuracy—can propagate errors in simulated outcomes. Future research should explore the integration of agent-based modeling, socio-economic datasets, and participatory scenario-building approaches to enrich simulation outputs and improve their policy relevance.

6. Conclusion and Policy-Oriented Recommendations

This study employed a CA–Markov-based modeling framework to simulate and forecast the dynamics of land use and land cover (LULC) in Sanandaj over the 2020–2040 period. The findings reveal a systemic, nonlinear transformation of the regional landscape—marked by the collapse of traditional agricultural zones, the retreat of barren lands, temporary contraction of urban footprints, and a substantial rise in grassland/shrubland mosaics. These spatial shifts highlight both ecological processes and socio-economic inertia, reflecting the cumulative effects of policy gaps, unplanned urbanization, and environmental stressors. The simulated patterns of rewilding—whether passive or policy-driven—are not necessarily a sign of successful environmental management but may represent socio-economic fatigue, agricultural decline, and spatial fragmentation. The disappearance of croplands and the fluctuating urban footprints expose the vulnerability of anthropocentric land systems when detached from ecological thresholds and long-term planning. To address these challenges, the study identifies critical policy implications and strategic pathways:

1. Protection and Revitalization of Agricultural Landscapes: With cropland projected to decline by more than 94%, urgent interventions are needed to halt rural land abandonment and food insecurity. Recommended measures include:
- Land tenure reforms and financial incentives for sustainable agriculture.
- Deployment of water-efficient irrigation technologies (e.g., drip irrigation, aquifer recharge).
- Agro-ecological zoning to protect high-yield farmlands from urban encroachment.
- Farmer-support programs and subsidies target climate-resilient crops.

2. Reframing Urbanization Trajectories: The observed and projected contraction of built-up areas suggests the need for rethinking urban development strategies:
- Prioritize compact, vertical urbanism rather than horizontal sprawl.
- Enforce geomorphologically informed zones to prevent construction in fragile zones (e.g., steep slopes, flood-prone areas).
- Introduce urban growth boundaries (UGBs) and smart-growth policies to optimize land efficiency.

3. Ecological Restoration and Rewilding Initiatives: The 81% increase in grassland/shrubland offers opportunities for ecosystem recovery:
- Implement structured rewilding programs incorporating native species and ecological corridors.
- Establish carbon sequestration projects and biodiversity hotspots on abandoned croplands.
- Integrate these landscapes into regional climate adaptation and mitigation strategies.

4. Adaptive Water and Wetland Governance: Hydrological dynamics, including the appearance of new wetlands, demand adaptive governance:
- Design watershed-level management plans with community participation.
- Promote small-scale water retention structures, artificial wetlands, and aquifer recharge.
- Strengthen monitoring frameworks for water quality and availability under climate stress.

5. Integrated and Multi-Scenario Land Use Modeling: While the CA–Markov model has proven valuable, it lacks socio-economic and institutional dimensions. Future studies should:
- Combine CA–Markov with Agent-Based Models (ABM) or Artificial Neural Networks (ANN) to simulate human decision-making.
- Utilize participatory scenario planning to incorporate local knowledge and policy perspectives.
- Develop multi-model frameworks that integrate climate projections, socio-economic drivers, and policy simulations.

Based on the modeling outcomes, three policy scenarios emerge for Sanandaj's future landscape:
- **Scenario A – Business-as-Usual (BAU):** Continuation of current trends, resulting in cropland loss, unplanned sprawl, and increasing ecological degradation.
- **Scenario B – Controlled Growth and Agro-Protection:** Implementation of urban containment policies and agricultural revitalization, balancing urban expansion with rural sustainability.
- **Scenario C – Eco-Centric Development:** Aggressive rewilding, forest regeneration, and smart urban densification, transforming Sanandaj into a climate-resilient and biodiversity-rich urban system.

In sum, Sanandaj stands at a critical crossroads—between ecological recovery and socio-economic vulnerability. Whether this transformation leads to a resilient landscape mosaic or devolves into unmanaged entropy will depend on the timely implementation of science-informed, inclusive, and forward-looking governance frameworks.

7. Declarations
7.1. Conflict of Interest
Authors declare that they have no known competing financial interests or personal relationships that could have appeared to influence the work reported in this paper.

7.2. Funding
Authors confirm that they have not received any funding or financial support from public, private, or

non-profit organizations for the conduct or publication of this research.

7.3. Author Contribution
Akbar Heydari: Conceptualization, Data Curation & Writing.
Mohsen Janparvar: Methodology & Software.
Mohammad Ali Gholami Sefidkouhi: Formal Analysis & Visualization.
Shadieh Heydari: Original draft & Review & Editing.

7.4. Publication Statement
This manuscript has not been published previously and is not under consideration for publication elsewhere. The author has read and approved the final version of the manuscript.

References

1. Alavipanah, S. K., Joolaei, A., & Zare, M. (2019). Environmental and climatic characteristics of mountainous cities in western Iran. Journal of Mountain Geography, 7(2), 45–5
2. Al-shalabi, M., et al. (2013). Prediction of land use/land cover changes using Markov-CA. The International Archives of the Photogrammetry, Remote Sensing and Spatial Information Sciences, 40(2), 283.
3. Baker, J. L., & McKinsey, D. J. (2021). Urbanization and food systems in the Middle East and North Africa: Trends, challenges and options. World Bank Publications.
4. Batisani, N., & Yarnal, B. (2009). Uncertainty awareness in urban sprawl simulations: A case study from the Susquehanna River Basin. Geoforum, 40(4), 581–59. https://doi.org/10.1016/j.geoforum.2009.03.007.
5. Chen, G., Hay, G. J., Carvalho, L. M. T., & Wulder, M. A. (2012). Object-based change detection. International Journal of Remote Sensing, 33(14), 4434–4457. https://doi.org/10.1080/01431161.2011.649831
6. Chen, X., & Pontius, R. G. (2010). Diagnostic tools to evaluate a spatial land change projection along a gradient of an explanatory variable. Landscape and Urban Planning, 94(1), 1–9. https://doi.org/10.1016/j.landurbplan.2009.07.006
7. Eastman, J. R. (2012). IDRISI Selva: Guide to GIS and image processing. Clark University.
8. Fan, F., Weng, Q., & Wang, Y. (2007). Land use and land cover change in Guangzhou, China, from 1998 to 2003, based on Landsat TM/ETM+ imagery. Sensors, 7(7), 1323–1342. https://doi.org/10.3390/s7071323.
9. Foley, J. A., et al. (2005). Global consequences of land use. Science, 309(5734), 570–574. https://doi.org/10.1126/science.1111772.
10. Hansen, M. C., et al. (2013). High-resolution global maps of 21st-century forest cover change. Science, 342(6160), 850–853. https://doi.org/10.1126/science.1244693.
11. Hyandye, C. B., & Martz, L. W. (2017). A Markov-based cellular automata model for land use change simulation. Geocarto International, 32(9), 957–978. https://doi.org/10.1080/10106049.2016.1188163
12. Iranian Meteorological Organization. (2020). Annual climate report of Kurdistan province. Tehran: IMO Publications.
13. Jat, M. K., Garg, P. K., & Khare, D. (2008). Monitoring and modelling of urban sprawl using remote sensing and GIS techniques. International Journal of Applied Earth Observation and Geoinformation, 10(1), 26–43.
14. Javadi, H., Mohammadi, M., & Zarei, S. (2021). Spatial simulation of land use change using CA–Markov model in western Iran. Journal of Environmental Management and Planning, 23(1), 103–118.
15. Kalnay, E., & Cai, M. (2003). Impact of urbanization and land-use change on climate. Nature, 423(6939), 528–531. https://doi.org/10.1038/nature01675
16. Kamusoko, C., et al. (2009). Simulating urban growth using GIS and remote sensing: A case study of Harare Metropolitan Province, Zimbabwe. Environment and Planning B: Planning and Design, 36(2), 230–249.
17. Karimi, A., & Gharakhlou, M. (2017). Urban network analysis of Kurdish cities in western Iran. Iranian Journal of Regional Planning, 7(1), 35–52.
18. Lambin, E. F., & Geist, H. J. (2006). Land-use and land-cover change: Local processes and global impacts. Springer Science & Business Media.
19. Liu, Y., et al. (2020). Urban expansion simulation and the spatiotemporal pattern of land use transitions. Sustainability, 12(3), 1025. https://doi.org/10.3390/su12031025
20. Liu, Y., Wang, J., Long, H., & Li, Y. (2012). Spatio-temporal analysis of land-use conversion in

urban fringe areas: A case study of Bejing, China. Habitat International, 36(4), 542–550. https://doi.org/10.1016/j.habitatint.2012.03.005

21. Mafi-Gholami, D., Amini, P., & Rezaei, M. (2022). Evaluating urban expansion and land degradation in Sanandaj using remote sensing and landscape metrics. Environmental Monitoring and Assessment, 194, Article 214. https://doi.org/10.1007/s10661-022-09823-x
22. Nivedita, G., Singh, S. K., & Prasad, R. (2018). Performance comparison of image classification techniques for land use/land cover mapping. Geocarto International, 33(10), 1019–1039. https://doi.org/10.1080/10106049.2017.1316770
23. Nouri, J., & Riazi, R. (2018). Spatial inefficiencies in urban land use planning: The case of Sanandaj. Urban Management Studies, 10(4), 65–82.
24. Pontius, R. G., & Malanson, J. (2005). Comparison of the structure and accuracy of two land change models. International Journal of Geographical Information Science, 19(2), 243–265.
25. Rahimi, M., Asgari, A., & Taghipour, A. (2018). Analyzing land use changes in mountainous cities of Iran: A focus on ecological constraints. Journal of Geography and Urban Planning, 12(3), 22–37.
26. Rahnama, M. R., & Farjad, B. (2015). Modeling urban expansion using a CA–Markov model in a GIS environment: A case study of Sanandaj City, Iran. Environmental Earth Sciences, 74(8), 5905–5918. https://doi.org/10.1007/s12665-015-4609-1
27. Saeidi, M. (2020). The impact of rural-to-urban migration on urban expansion in Sanandaj. Geographical Research Quarterly, 35(2), 97–112.
28. Sangermano, F., Toledano, J., & Eastman, J. R. (2012). Land cover change in the Bolivian Amazon and its implications for REDD+ and endemic biodiversity. Landscape Ecology, 27(4), 571–584. https://doi.org/10.1007/s10980-012-9710-y.
29. Sangermano, F., Toledano, J., & Eastman, J. R. (2012). Land cover change in the Bolivian Amazon and its implications for REDD+ and endemic biodiversity. Landscape Ecology, 27(4), 571–584. https://doi.org/10.1007/s10980-012-9710-y
30. Seto, K. C., Güneralp, B., & Hutyra, L. R. (2012). Global forecasts of urban expansion to 2030 and direct impacts on biodiversity and carbon pools. Proceedings of the National Academy of Sciences, 109(40), 16083–16088.
31. Seto, K. C., Güneralp, B., & Hutyra, L. R. (2012). Global forecasts of urban expansion to 2030 and direct impacts on biodiversity and carbon pools. Proceedings of the National Academy of Sciences, 109(40), 16083–1608.
32. Shabani, F., & Bakhtiari, H. (2021). Predicting future land use and land cover changes using CA–Markov and machine learning models: Case study of Sanandaj, Iran. Sustainable Cities and Society, 67, 102748. https://doi.org/10.1016/j.scs.2020.10274
33. Singh, S. K., & Glenn, N. F. (2009). Multiscale modeling of landscape dynamics. In Land Change Science in the Tropics (pp. 305–320). Springer.
34. Singh, S. K., & Glenn, N. F. (2009). Multiscale modeling of landscape dynamics. In Land Change Science in the Tropics (pp. 305–320). Springer.
35. Sohl, T. L., & Claggett, P. R. (2013). Clarity versus complexity: Land-use modeling as a practical tool for decision-makers. Journal of Environmental Management, 129, 235–243. https://doi.org/10.1016/j.jenvman.2013.07.027
36. Sohl, T. L., & Claggett, P. R. (2013). Clarity versus complexity: Land-use modeling as a practical tool for decision-makers. Journal of Environmental Management, 129, 235–243. https://doi.org/10.1016/j.jenvman.2013.07.027
37. Statistical Center of Iran. (2021). Statistical Yearbook of Kurdistan Province 2020. Tehran: SCI Publications.
38. Turner, B. L., Lambin, E. F., & Reenberg, A. (2007). The emergence of land change science for global environmental change and sustainability. Proceedings of the National Academy of Sciences, 104(52), 20666–20671.
39. Verburg, P. H., de Koning, G. H., Kok, K., Veldkamp, A., & Bouma, J. (1999). A spatial explicit allocation procedure for modelling the pattern of land use change based upon actual land use. Ecological Modelling, 116(1), 45–61. https://doi.org/10.1016/S0304-3800(98)00156-2.
40. Zhao, H., Li, X., & Wang, H. (2021). Assessing land use change using high-resolution Sentinel-2 imagery and Markov model. Remote Sensing, 13(14), 2774. https://doi.org/10.3390/rs13142774.